

# Cloning and expression of the gene encoding the *Thermoanaerobacter ethanolicus* 39E secondary-alcohol dehydrogenase and biochemical characterization of the enzyme

Douglas S. BURDETTE\*, Claire VIEILLE\* and J. Gregory ZEIKUS\*†‡

\*Biochemistry Department, Michigan State University, East Lansing, MI 48824, U.S.A., and †Michigan Biotechnology Institute, 3900 Collins Road, Lansing, MI 48910, U.S.A.

The *adhB* gene encoding *Thermoanaerobacter ethanolicus* 39E secondary-alcohol dehydrogenase (S-ADH) was cloned, sequenced and expressed in *Escherichia coli*. The 1056 bp gene encodes a homotetrameric recombinant enzyme consisting of 37.7 kDa subunits. The purified recombinant enzyme is optimally active above 90 °C with a half-life of approx. 1.7 h at 90 °C. An NADP(H)-dependent enzyme, the recombinant S-ADH has 1400-fold greater catalytic efficiency in propan-2-ol oxidation than in ethanol oxidation. The enzyme was inactivated by chemical modification with dithionitrobenzoate (DTNB) and diethylpyrocarbonate, indicating that Cys and His residues are involved in catalysis. Zinc was the only metal enhancing S-ADH reactivation after DTNB modification, implicating the involvement of bound zinc in catalysis. Arrhenius plots for the oxidation

of propan-2-ol by the native and recombinant S-ADHs were linear from 25 to 90 °C when the enzymes were incubated at 55 °C before assay. Discontinuities in the Arrhenius plots for propan-2-ol and ethanol oxidations were observed, however, when the enzymes were preincubated at 0 or 25 °C. The observed Arrhenius discontinuity therefore resulted from a temperature-dependent, catalytically significant S-ADH structural change. Hydrophobic cluster analysis comparisons of both mesophilic and thermophilic S-ADH and primary- versus S-ADH amino acid sequences were performed. These comparisons predicted that specific proline residues might contribute to S-ADH thermostability and thermophilicity, and that the catalytic Zn ligands are different in primary-alcohol dehydrogenases (two Cys and a His) and S-ADHs (Cys, His, and Asp).

## INTRODUCTION

Alcohol dehydrogenases (ADHs) [EC 1.1.1.1 (NADH) or EC 1.1.1.2 (NADPH)] have been well studied as a structurally conserved class of enzyme [1]. The X-ray structure of the horse liver primary-alcohol dehydrogenase (P-ADH) is known, and the properties of this enzyme have been extensively detailed [1,2]. ADHs are typically dimeric or tetrameric pyridine dinucleotide-dependent metalloenzymes with a zinc atom involved in catalysis. ADHs have been classified as P-ADHs or secondary-alcohol dehydrogenases (S-ADHs) on the basis of their relative activities towards primary and secondary alcohols. It generally has been assumed that P-ADHs and S-ADHs are structurally similar and that their substrate differences are due to relatively small changes in their active site architecture. Tetrameric S-ADHs have been reported from a number of micro-organisms [3–7]. The *Thermoanaerobacter ethanolicus* 39E S-ADH is a bifunctional ADH/acetyl-CoA reductive thioesterase [7]. It has been proposed to function physiologically by oxidizing nicotinamide cofactor during ethanol formation, indirectly preventing glycolytic inhibition at the glyceraldehyde dehydrogenase step [8].

S-ADHs are attractive subjects for research into chiral chemical production because of their broad specificities and their highly enantiospecific conversion of prochiral ketones to alcohols [9–12].

Two issues facing the commercial-scale application of S-ADHs in chiral syntheses are the difficulty of regenerating and retaining expensive nicotinamide cofactor and the lack of inexpensive, highly stable enzymes. Cofactor regeneration and retention have been overcome by numerous strategies [13,14]. Although thermophilic enzymes are generally much more stable than their mesophilic counterparts, the organisms that produce thermophilic S-ADHs grow slowly and to low cell densities, making an alternative expression system for these enzymes crucial for both their commercial application and detailed protein structure–function studies.

The discovery of thermophilic bacteria has provided the opportunity to isolate thermostable enzymes directly. The thermophilic anaerobes *T. ethanolicus* and *T. Brockii* [15] express extremely enantiospecific S-ADHs that are stable above 70 °C. These two S-ADHs have been proposed to be extremely structurally similar on the basis of similar molecular masses and kinetic characteristics [16]. Although the *Clostridium beijerinckii* gene (*adhB*) encoding a mesophilic NADP(H)-dependent S-ADH has been cloned and sequenced (GenBank accession no. M84723), and although the amino acid sequence of the *T. Brockii* S-ADH has been determined by Edman degradation [17], no cloned thermophilic S-ADH is available for detailed biochemical studies.

Abbreviations used: ADH, alcohol dehydrogenase; DTNB, dithionitrobenzoate; DEPC; diethylpyrocarbonate; HCA, hydrophobic cluster analysis; DTT, dithiothreitol; MALDI, matrix-associated laser desorption ionization mass spectrometry; ORF, open reading frame; P-ADH, primary-alcohol dehydrogenase; RBS, ribosome binding site; S-ADH; secondary-alcohol dehydrogenase.

‡ To whom correspondence should be addressed. Present address: Biochemistry Department, Michigan State University, East Lansing, MI 48824, U.S.A.

The nucleotide sequence reported will appear in DDBJ, EMBL and GenBank Nucleotide Sequence Databases under the accession number U49975.

The work reported here describes the cloning, sequencing and expression of the gene encoding the thermophilic *T. ethanolicus* S-ADH. The kinetic and thermal properties of the recombinant enzyme are determined. The biochemical basis for the enzyme's discontinuous Arrhenius plots is investigated. Finally, the protein sequence information is used to examine the structural similarities between thermophilic and mesophilic P-ADHs and S-ADHs. These comparisons are used to predict the S-ADH catalytic Zn liganding residues and the potential involvement of specific prolines in the thermal stability of S-ADH.

## MATERIALS AND METHODS

### Chemicals and reagents

All chemicals were of at least reagent/molecular biology grade. Gases were provided by AGA Specialty Gases (Cleveland, OH, U.S.A.) and made anaerobic by passage through heated copper filings. Oligonucleotide syntheses and amino acid sequence analyses were performed by the Macromolecular Structure Facility (Department of Biochemistry, Michigan State University). The kanamycin resistance GenBlock (*EcoRI*) DNA cartridge used in expression vector construction was purchased from Pharmacia (Uppsala, Sweden) [18].

### Media and strains

*T. ethanolicus* 39E (ATCC no. 33223) was grown in TYE medium as previously described [19]. All batch cultures were grown anaerobically under a nitrogen gas headspace. *Escherichia coli* DH5 $\alpha$  containing the recombinant *adhB* gene was grown in rich complex medium (20 g/l tryptone, 10 g/l yeast extract, 5 g/l NaCl) at 37 °C in the presence of 25  $\mu$ g/ml kanamycin and 100  $\mu$ g/ml ampicillin.

### DNA manipulations and library construction

Plasmid DNA purification, restriction analysis, PCR and colony and DNA hybridizations were performed with conventional techniques [20,21]. *T. ethanolicus* chromosomal DNA was purified as previously described [22]. Partly digested 2–5 kb *Sau3AI* fragments were isolated by size fractionation from a 10–40% sucrose gradient [20] and ligated into pUC18 *BamHI*/BAP (Pharmacia, Uppsala, Sweden). The ligation mixture was transformed into *E. coli* DH5 $\alpha$  by electroporation [21]. Degenerate primers (1) [5'-ATGAA(R)GG(N)TT(H)GC(N)ATG(Y)T] and (2) [5'-G(W)(N)GTCATCAT(R)TC(N)G(K)(D)ATCAT] were used to synthesize the homologous probe for colony hybridization [23]. The DNA fragment containing the *adhB* gene was sequenced by the method of Sanger et al. [24].

### Enzyme purification

The native S-ADH was purified by established techniques [7]. The recombinant enzyme was purified from *E. coli* DH5 $\alpha$  aerobically. The pelleted cells from batch cultures were resuspended (0.5 g wet wt. per ml) in 50 mM Tris/HCl, pH 8.0, (buffer A) containing 5 mM dithiothreitol (DTT), and 10  $\mu$ M ZnCl<sub>2</sub>, and lysed by passage through a French pressure cell. The clarified lysate was incubated at 65 °C for 25 min and then centrifuged for 30 min at 15000 *g*. The supernatant was applied to a DEAE-Sephacryl column (2.5 cm  $\times$  15 cm) that had been equilibrated with buffer A and eluted with a 250 ml NaCl gradient (0–300 mM). Active fractions were diluted 4-fold in buffer A and applied to a Q-Sepharose column (2.5 cm  $\times$  10 cm)

equilibrated with buffer A. Purified enzyme was eluted with a 250 ml NaCl gradient (0–300 mM).

### Molecular mass determination

Recombinant holoenzyme molecular mass was determined by comparison with protein standards (Sigma, St. Louis, MO, U.S.A.) by gel filtration chromatography (0.5 ml/min) with a Pharmacia S300 column (110 cm  $\times$  1.2 cm) equilibrated with buffer A containing 200 mM NaCl. Subunit molecular mass values were determined by matrix-associated laser desorption ionization mass spectrometry (MALDI) at the Michigan State University Mass Spectrometry Facility.

### Kinetics and thermal stability

The standard S-ADH activity assay was defined as NADP<sup>+</sup> reduction coupled to propan-2-ol oxidation at 60 °C as previously described [7]. The enzyme was incubated at 55 °C for 15 min before activity determination unless otherwise indicated. Assays to determine  $K_m$  (app) and  $V_{max}$  (app) were conducted at 60 °C with substrate concentrations between 20 $K_m$  (app) and 0.2 $K_m$  (app). Kinetic parameters were calculated from nonlinear best fits of the data to the Michaelis–Menten equation by using Kinzyme software [25]. Protein concentrations were measured by the bicinchoninic acid procedure (Pierce, Rockford, IL, U.S.A.) [26].

S-ADH thermostability was measured as the residual activity after timed incubation at the desired temperatures. Thermal inactivation was stopped by incubation for 30 min at 25 °C, and samples were prepared for activity assays by preincubation at 55 °C for 15 min. Incubations were performed in 100  $\mu$ l PCR tubes (Sarstedt cat. no. 72.733.050; Newton, NC, U.S.A.) with 200  $\mu$ g/ml protein in 100  $\mu$ l of buffer A. Activity was determined in the unfractionated samples. The temperature effect on enzyme activity was studied with the substrates propan-2-ol or ethanol at 10 $K_m$  (app) concentrations.

To study the effect of enzyme preincubation temperature on enzyme reaction rates, the S-ADH was incubated at 0, 25 or 55 °C for 15 min before activity determinations in the temperature range 30–90 °C. Tris/HCl buffer pH values were adjusted at 25 °C to be pH 8.0 at the temperature they were used (with a thermal correction factor of  $-0.031\Delta\text{pH}/^\circ\text{C}$ ). The statistical significance of the differences between the Arrhenius plot slopes above and below the discontinuity temperatures was determined by covariance analysis [27].

### Chemical modification

Cysteine residues were reversibly modified with dithionitrobenzoate (DTNB) at 25 and 60 °C [28]. DTNB-inactivated S-ADH was reactivated with DTT in the presence of 0.01–1.0 mM metal salts or 0.5–3.0 mM EDTA. Histidine residues were chemically modified with diethylpyrocarbonate (DEPC) by incubation with 20 mM or 40 mM DEPC in 50 mM phosphate buffer, pH 6.0, at 25 °C for 1.0 h and the reaction was quenched by the addition of 0.5 vol. of 0.5 M imidazole, pH 6.5 [29].

### Protein sequence comparisons

The peptide sequences of the *Bacillus stearothermophilus* (accession no. D90421), *Sulfolobus solfataricus* (accession no. S51211) and *Zymomonas mobilis* (accession no. M32100) P-ADHs and of the *Alcaligenes eutrophus* (accession no. J03362) and *Clostridium beijerinckii* (accession no. M84723) S-ADHs were obtained from GenBank. The horse liver P-ADH [1] and

the *T. brockii* S-ADH [17] peptide sequences were obtained from the literature. Access to GenBank, standard sequence alignments and percentages of amino acid similarity/identity were performed with the Program Manual for the Wisconsin Package, Version 8, Sept. 1994 (Genetics Computer Group, Madison, WI, U.S.A.). Protein sequence alignments were performed by hydrophobic cluster analysis (HCA) [30]. HCA plots of individual protein sequences were generated with HCA-Plot V2 computer software (Doriane, Le Chesnay, France).

**RESULTS**

**Cloning and sequencing of the *T. ethanolicus adhB* gene**

The *T. ethanolicus* S-ADH was cloned from a *T. ethanolicus* chromosomal DNA library by homologous hybridization. The N-terminal sequence of the native *T. ethanolicus* S-ADH (MKG FAML) was identical with those of *C. beijerinckii* and *T. brockii* S-ADHs. This sequence was used to generate primer (1). Alignment of the *C. beijerinckii* and *T. brockii* S-ADH peptide sequences indicated another conserved region (residues 147–153) that would reverse translate into a low-degeneracy oligonucleotide [primer (2)]. The PCR product obtained with primers (1) and (2), and with *T. ethanolicus* chromosomal DNA as the template, was 470 bp, as expected from the position of primers (1) and (2) in the *C. beijerinckii* and *T. brockii* S-ADHs. This PCR product was used as a homologous probe to screen the *T. ethanolicus* genomic library. The positive clone showing the highest S-ADH activity at 60 °C was selected for further studies. Plasmid pADHB25-C contained a 1.6 kb *Sau3AI* insert and was shown by subsequent sequencing and peptide analyses to carry the complete *adhB* gene. The 1.6 kb insert was subcloned into the pBluescriptIIKS(+) *XbaI* site to construct the expression plasmid pADHB25. The physical map of pADHB25 is shown in Figure 1. Plasmid pADHB25 was stabilized by insertion of a kanamycin resistance cartridge into the vector *EcoRI* site, allowing dual selection on kanamycin and ampicillin. This final construct (pADHB25-kan) was used for all subsequent work.

The nucleotide sequence of the pADHB25 insert is shown in Figure 2. A unique open reading frame (ORF) was identified that encoded a polypeptide that was highly similar to *C. beijerinckii* S-ADH and started with the N-terminal sequence of the native *T. ethanolicus* S-ADH. Two consecutive ATG codons were identified as potential translation initiation codons. The N-terminus of the native S-ADH starts with a single Met, suggesting that the first ATG codon is not translated or is removed post-translationally. A potential ribosome binding site (RBS) (positions 223–228) is located 10 bp upstream of the start codon. A

```

90
TGACAATAGACAACCCCTTCTGTGATCTGTTTTTTCGAAATGCTATTTTACACAAGAGATTCTCTAGTCTTTTACTTAAAA
180
AACCCGTACGAATTTTAACTATCTCGAATAAATTTGATATTTTAACTATGCTTATTAATTTGCAAAAAATTAACAAATCAT
-35
-10
CGCGTAAGCTAGTTTTCACATTAATGACTTACCCAGTATTTAGGAGCTTTTAAATGATGAAAGTTTGAACCTCAGTATCGGTAAA
RBS MKGFAMLSIGK
360
GTGTGGTGGATGAGAAGAAAACCGCTCTCTGGCCCATTTGATGCTATTGAGACCTCTAGCTGTGGCCCTTGCACCTCGGACATT
V G W I E K E K P A P G P F D A I V R P L A V A P C T S D I
450
CATACCGTTTGAAGGAGCCATTGGCGAAGACATAACATGATACTCGTCCAGCAAGCTAGGTGAGTAGTGTGAAGTAGTGTAGT
H T V F E G A I G E R H N M I L G H E A V G E V V E V G S E
540
GTAAGAATTTAAACCTGTGATGCGCTTGTGTGCCAGCTATTACCCCTGATTGTGGACCTCTGAGTACAAAGAGATATCACCCAG
V K D F K P G D R V V V P A I T P D W W T S E V Q R G Y H Q
630
CACTCGGTGGAATGCTGGCAGCTGGAATTTTGAATGTAAGAAGTGTGTTTTGTTGTAATTTTTCATGTGAATGATCGCTGATG
H S G G M L A G W K F S N V K D G V F G E F F H V N D A D M
720
AATTAGCAGCTGCCTAAGAAATTCATTTGGAAGCTGCAATGATTCGCCGATATGATGACCACTGTTTCACCGAGCTGAECT
N L A H L P K E I P L E A A V M I P D M M T T G F H G A E L
810
GCAGATAGAAATAGTGGCAGGAGTACGATTTGGGATTTGGCCAGTAGGCTTATGGCAGTCCGCTGTCGCAATTCGCTGGAGCC
A D I E L G A T V A V L G I G P V G L M A V A G A K L R G A
900
GGAGAATTTGCGGTAGCAGTACCACTTTGTTAGATGCTGCAAAATACATGAGGACTACTGATTTGTAACCTATAAAGATGCT
G R I I A V G S R P V C V D A A K Y G A T D I V N Y K D G
990
CCTATGGAATGATGATTAAGAACTAAGTCAAGGCAAGGCTGCGATGCTGCCATTCGCTGGAGAAATCCTGACATTTAGGCTACA
P I E S Q I M N L T E G K G V D A A I I A G G N A D I M A T
1080
GCAGTAAAGATTTAACTGGTGGCACCATCGCTAATGAAATTTTGGGCAAGGAGAGGTTTTCCTGCTCTCTGCTTGAATGG
A V K I V R P G G P I A N V N Y P G E G E V L P V P R L E W
1170
GGTGGCAGTGCCTATAAATGAGGCGGCTATCCCGGCGAGCTTAAAGATGGAAGACTGATGACCTTTTGTAT
G C G M A H K T I K G G L C P F G R L M R E R L I D L V F T
1260
AAGCCTGCGATCTCTAGCTCTGCTCACTCAGCTTTTCGAGGATTTGCAATATTTGAAAGCCCTTATGTTGTAAGAGACAAACCA
K P V D P S K L V T H V F Q G F D N I E K A F M L M K D K P
1350
AAAGCAATCAACCTGTTGTAATTTAGCATAAATGGGACCTAGTCCATTTTATGCTAATAGGCTAAATACACTGGTGT
K D L I K P V V I L A ***
1440
TATATGACACATCGGCCAGTAACTCTGGTAAAAAATAACAAAAATAGTATTTTCTTAACATTTTACCGCATTAACACTGTATA
1530
CATCATGAAGAAAGTAAATAACAACCTATTAATAAAGAGAGAGGAGGATTTATCATGTCAAAATTTAGAAAAAGAGAAATGGCACC
RBS M F K I L E K R E L A P
1620
TTCCATAGGTTGTTGATATAGAGCACCAGTACGCAAAAGCAGGCGCCCAATTCGTTATGCTAAGCAATMAAGAGGCGG
S I K L F V I E A P L V A K K A R P G N F V M L R I K E G G
AGAAGAATT 1630
E R I
    
```

**Figure 2** Nucleotide sequence and deduced amino acid sequence of *T. ethanolicus* 39E *adhB* and of the downstream ORF

The putative promoter –35 and –10 regions and RBSs are underlined. The *adhB* stop codon is indicated by three asterisks.

potential promoter was identified approx. 70–100 bp upstream of the RBS. The ‘–35’ and ‘–10’ regions are highly similar to the *E. coli* consensus promoter sequences [31], and are separated by 16 bp. The ‘–10’ region is duplicated, with the second copy overlapping the first. Because of its incorrect distance from the ‘–35’ region, this second copy may only provide an A+T-rich sequence to aid in strand separation. No transcriptional stop site was identified downstream of *adhB*. In this region, instead, a truncated ORF, preceded by an RBS, was identified. It translated into a 45 amino acid peptide fragment 46% identical and 68% similar to the product of a similar truncated ORF located downstream of the *C. beijerinckii adhB* gene. Little similarity was found with other sequences in GenBank, so the function of this ORF remains unknown.

**Sequence comparison of P-ADHs and S-ADHs**

Standard alignments of P-ADH and S-ADH amino acid sequences indicated a high level of similarity between the three S-ADHs from obligate anaerobes (Table 1). The *T. ethanolicus* S-ADH differed from the *T. brockii* enzyme by only three residues, and was 75% identical with the enzyme from the mesophile *C. beijerinckii*. The similarity was lower for comparisons with the S-ADH from the obligate aerobe *A. eutrophus*. The P-ADHs showed less sequence conservation (25–54% identity and 49–71% similarity) than the S-ADHs, and showed only 20–27% identity (and 48–51% similarity) with the S-ADHs. Based on these standard alignments, the conservation of important core

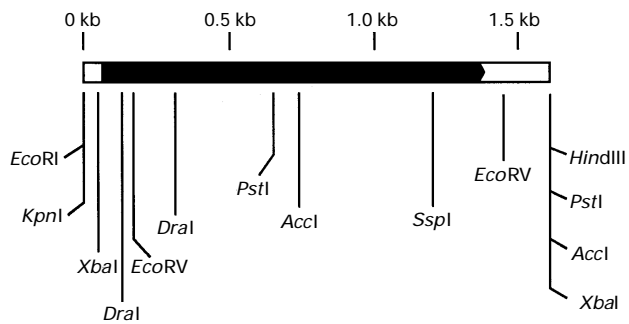


**Figure 1** Restriction map of the *T. ethanolicus* 39E S-ADH clone (pADHB25)

The flanking restriction sites are from the plasmid polylinker.

**Table 1 Comparison of primary structural similarity between horse liver and bacterial alcohol dehydrogenases**

Percentage identities and similarities were calculated by the GCG Gap program with penalties for gap insertion (3.0) and extension (0.1). Abbreviations used: *T. eth*, *T. ethanolicus* 39E; *T. bro*, *T. brockii*; *C. bei*, *C. beijerinckii*; *A. eut*, *A. eutrophus*; *B. stea*, *B. stearothermophilus*; *S. sul*, *S. solfataricus*; *Z. mob*, *Z. mobilis*; liver, horse liver.

	Identity (similarity) of sequence (%) with sequences from the following organisms:							
	<i>T. eth</i>	<i>T. bro</i>	<i>C. bei</i>	<i>A. eut</i>	<i>B. stea</i>	<i>S. sul</i>	<i>Z. mob</i>	Liver
S-ADHs:								
<i>T. eth</i> *	100							
<i>T. bro</i> *	99.1 (99.4)	100						
<i>C. bei</i>	74.4 (86.6)	75.0 (86.9)	100					
<i>A. eut</i>	35.6 (61.5)	36.2 (62.1)	36.2 (59.5)	100				
P-ADHs:								
<i>B. stea</i> *	26.7 (50.6)	27.2 (50.8)	24.1 (50.6)	31.9 (53.8)	100			
<i>S. sul</i> *	27.0 (51.6)	26.4 (51.0)	24.0 (50.6)	25.8 (49.0)	35.2 (55.8)	100		
<i>Z. mob</i>	24.2 (48.2)	25.1 (48.8)	20.5 (48.4)	25.6 (51.2)	54.0 (71.0)	33.9 (54.6)	100	
Liver	28.8 (53.8)	29.1 (54.4)	27.4 (52.6)	23.1 (49.7)	32.8 (55.4)	28.9 (50.9)	31.1 (50.4)	100

\*: Thermophilic Adh.

domain residues, amino acids lining the active site pocket, and structurally conserved glycines identified for the horse liver enzyme [1] was higher in all the peptides.

HCA comparisons allow the alignment of potentially similar secondary or tertiary structural regions between enzymes with dissimilar amino acid sequences. The Rossmann fold consensus sequences, Gly-Xaa-Gly-Xaa-Xaa-Gly-(Xaa)<sub>18-20</sub> [negatively charged amino acid for NAD(H)-dependent or neutral amino acid for NAD(P)(H)-dependent] [32], identified in each of the ADH peptides were used to direct HCA alignments of P-ADHs and S-ADHs. Figure 3 shows a representative HCA multiple comparison between a thermophilic (*T. ethanolicus*) and a mesophilic (*C. beijerinckii*) S-ADH with a thermophilic (*B. stearothermophilus*) and a mesophilic (horse liver) P-ADH based on the identified Rossmann fold consensus sequences. The consensus motifs of the NADP(H)-linked *T. ethanolicus* and *C. beijerinckii* S-ADHs were identified as Gly<sup>174</sup>-Xaa-Gly<sup>176</sup>-Xaa-Xaa-Gly<sup>179</sup>, Gly<sup>198</sup>, and those of the NAD(H) dependent *B. stearothermophilus* and horse liver P-ADHs were identified as Gly<sup>172</sup>-Xaa-Gly<sup>174</sup>-Xaa-Xaa-Gly<sup>177</sup>, Asp<sup>195</sup> and Gly<sup>199</sup>-Xaa-Gly<sup>201</sup>-Xaa-Xaa-Gly<sup>204</sup>, Asp<sup>223</sup> respectively. This alignment also predicts 71–94% overall similarity between P-ADHs and S-ADHs for the critical hydrophobic core residues (71–94%), active site pocket residues (71–100%), and structurally critical glycines (100% in all cases) identified in the horse liver enzyme.

The HCA comparison allowed the identification of corresponding cluster regions and catalytically important residues in all four dehydrogenases on the basis of the corresponding residues identified for the horse liver enzyme [1,2]. The horse liver P-ADH contains two Zn atoms per subunit, one structural and one catalytic [1]. The thermophilic *B. stearothermophilus* P-ADH contained a region involving Cys residues 97, 100, 103 and 111 that is analogous to the structural Zn binding loop in the horse liver ADH (involving Cys<sup>92</sup>, Cys<sup>95</sup>, Cys<sup>98</sup> and Cys<sup>106</sup>). However, no analogous structural Zn binding loop regions were identified in the *T. ethanolicus* and *C. beijerinckii* S-ADHs (Figure 3). The catalytic Zn ligands in the horse liver enzyme have been established (Cys<sup>46</sup>, His<sup>68</sup> and Cys<sup>174</sup>). The N-terminal Cys and His ligands to the catalytic Zn atom appear to be conserved in both the P-ADH and S-ADH sequences (Figure 3). However, the second Cys ligand in the horse liver P-ADH (Cys<sup>174</sup>), conserved in the *B. stearothermophilus* P-ADH (Cys<sup>148</sup>), is replaced with an Asp residue (Asp<sup>150</sup>) in both the *T. ethanolicus* and *C. beijerinckii*

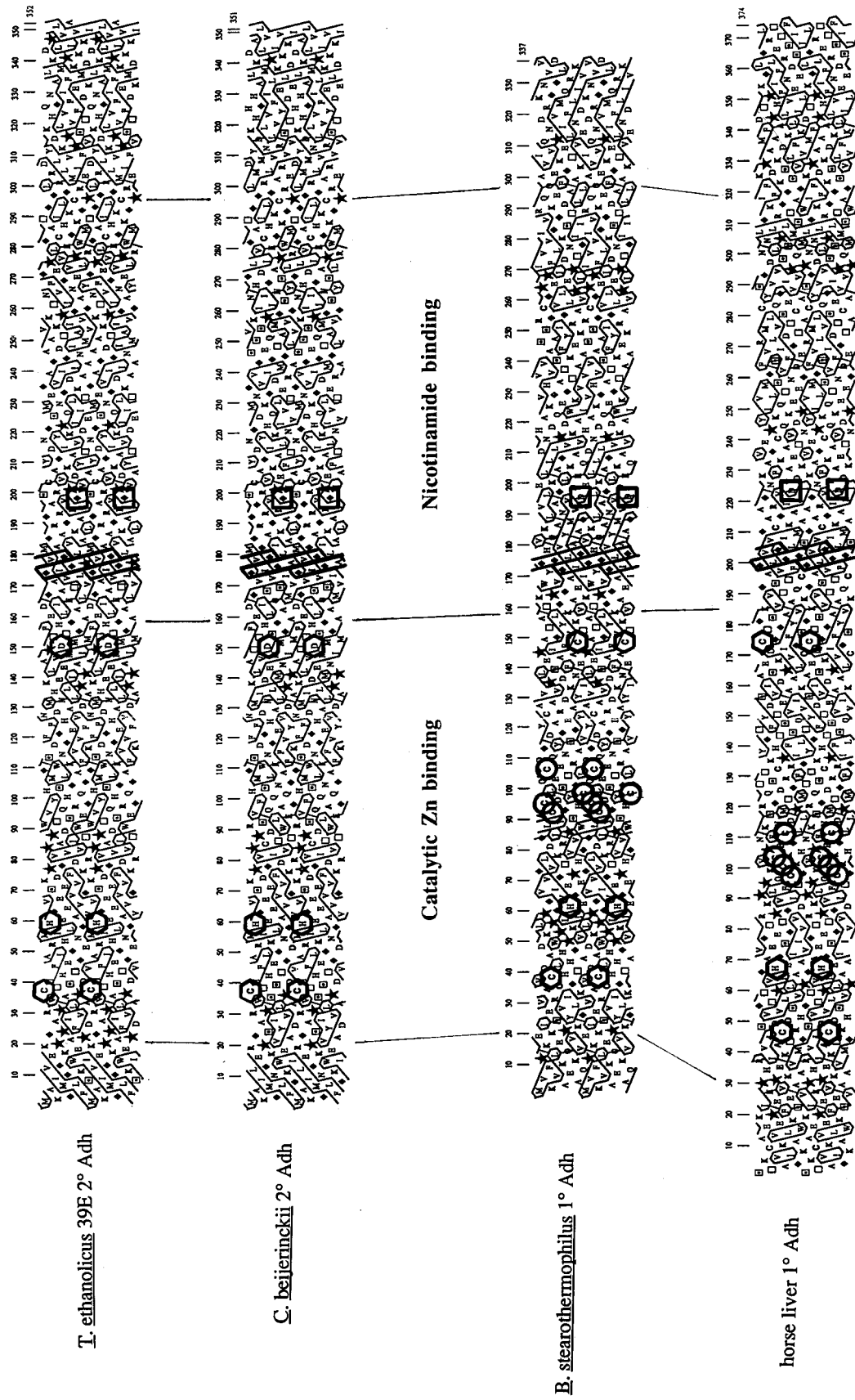
proteins. The *A. eutrophus* and *T. brockii* S-ADHs also conserved corresponding Asp residues and seemed to lack P-ADH-like structural Zn binding loops (results not shown).

#### Sequence comparison of S-ADH enzymes from a mesophile and thermophiles

The structural constraints introduced by proline residues have been proposed as a mechanism involved in protein thermostabilization [33]. Among the 12 non-conservative sequence substitutions between the mesophilic *C. beijerinckii* S-ADH and the thermophilic *T. ethanolicus* S-ADH, nine correspond to the introduction of prolines (22, 24, 149, 177, 222, 275, 313, 316 and 347) in the *T. ethanolicus* protein. All but Pro<sup>313</sup> are also present in the thermophilic *T. brockii* S-ADH. The mesophilic S-ADH subunit contains a total of 13 prolines (3.7%) whereas the *T. ethanolicus* and *T. brockii* subunits contain 22 prolines (6.2%) and 21 prolines (6.0%) respectively. Prolines 20, 22 and 24 are in a nine-residue stretch of hydrophilic amino acids near the putative catalytic Zn ligand Cys<sup>37</sup>. Pro<sup>149</sup> interrupts a hydrophobic cluster and is next to another putative Zn ligand, Asp<sup>150</sup>. The nicotinamide cofactor binding motif includes Pro<sup>177</sup>, which also interrupts a hydrophobic cluster region. Prolines 222, 275, 313, 316 and 347 are located in short (two to four residues) hydrophilic stretches that form putative turn regions.

#### Purification and characterization of the recombinant S-ADH

The recombinant *T. ethanolicus* S-ADH was highly expressed in *E. coli* in the absence of induction, and no significant increase was seen on induction with 5.0 mM isopropyl thio  $\beta$ -D-galactoside. The enzyme expression level was similar in *E. coli* and in the native organism (1–5% of total protein). The recombinant enzyme was purified 36-fold to homogeneity (as determined by the presence of a single band on SDS/PAGE). The subunit molecular masses were calculated from the average of three (native enzyme) and five (recombinant enzyme) determinations with MALDI, yielding masses for the native and recombinant enzyme subunits of 37707 and 37854 Da respectively. These values are within the generally accepted error of the technique (approx. 1%), and are in agreement with the theoretical molecular mass for the native enzyme based on the gene sequence (37644 Da). N-terminal amino acid analysis of the recombinant enzyme indicated that in  $72 \pm 5\%$  of the recombinant protein the



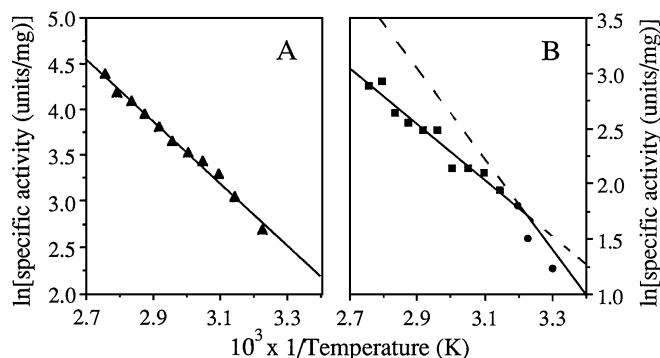


**Figure 4** Arrhenius plots for the recombinant *T. ethanolicus* 39E S-ADH between 25 and 90 °C

(A) Temperature–activity data for propan-2-ol oxidation with the enzyme preincubated at 55 °C. The linear regression best fit to the data was determined as  $y = 13.647 - 3.3694x$  ( $r^2 = 0.993$ ). (B) Temperature–activity data for ethanol oxidation with the enzyme preincubated at 55 °C. Points above and below the discontinuity are indicated by ■ and ● respectively. The linear regression best fits to the data were determined as  $y = 9.7929 - 2.5036x$  ( $r^2 = 0.946$ ) for points above and  $y = 15.730 - 4.3899x$  ( $r^2 = 0.969$ ) for points below the discontinuity.

two N-terminal ATG codons had been translated, whereas  $28 \pm 2\%$  of the protein contained a single N-terminal Met residue, like the native enzyme. The increased mass of 147 Da determined for the recombinant enzyme is consistent with the mass of one Met residue (149.2 Da), although this difference is small compared with the measurement error associated with MALDI. The recombinant holoprotein molecular mass was determined as 160 kDa by gel-filtration chromatography, demonstrating that the recombinant *T. ethanolicus* S-ADH, like the native enzyme, is a homotetramer.

The S-ADH was completely inactivated at both 25 and 60 °C by cysteine-specific DTNB modification. Inactivation was partially reversed at 60 °C by the addition of DTT, allowing the recovery of 34% of the initial activity (initial activity  $54 \pm 3.0$  units/mg). The addition of  $\text{CdSO}_4$ ,  $\text{FeCl}_2$ ,  $\text{MnCl}_2$ ,  $\text{CaCl}_2$ ,  $\text{MgCl}_2$ ,  $\text{NaCl}$  (0.01–1.0 mM) or EDTA (0.5–3.0 mM) did not affect enzyme reactivation by DTT, and the addition of  $\text{CoCl}_2$  or  $\text{NiCl}_2$  decreased the recovered activity to only 10% or 15%, respectively, of the initial activity. Zinc was the only metal to enhance the reactivation (up to 48% activity recovery in the presence of 100  $\mu\text{M}$   $\text{ZnCl}_2$ ). DEPC modification of histidine residues also completely inactivated the enzyme.

#### Characterization of thermal and kinetic properties of the recombinant *T. ethanolicus* S-ADH

The activity of the recombinant S-ADH towards ADH substrates was characterized. The  $V_{\text{max}}$  (app) for propan-2-ol (68 units/mg) was 3.6-fold higher than for ethanol (19 units/mg), and the  $K_m$  (app) towards the primary alcohol (53 mM) was almost 50-fold higher than for the secondary alcohol (1.1 mM). The catalytic efficiency of the recombinant enzyme was determined as approx. 170-fold greater towards the secondary alcohol (0.062 ml/min per mg) than towards the primary alcohol (0.00036 ml/min per mg). The  $K_m$  (app) for  $\text{NADP}^+$  was 0.011 mM, and no NAD(H)-dependent activity was detected. The temperature dependences of native and recombinant enzyme activities were determined as being similar. Thus only the results obtained with the recombinant enzyme are reported here. *T. ethanolicus* S-ADH activity was detected below 25 °C and increased to beyond 90 °C (Figure 4A). The S-ADH half-life at 90 °C was 1.7 h. The Arrhenius plot

**Table 2** Effect of enzyme preincubation temperature on the activation energy for 2-propanol and ethanol oxidation by *T. ethanolicus* 39E S-ADH

The existence of a biphasic Arrhenius plot was determined at the 95% confidence level by covariance analysis of the best-fit regression lines to the data.  $D$  is the activation energy below the discontinuity minus the activation energy above the discontinuity. Abbreviation used: N.D., not detectable (the rate discontinuity was statistically insignificant at the 95% confidence level).

Substrate	Preincubation temperature (°C)	Discontinuity temperature (°C)	Activation energy (kJ/mol)		$\Delta$
			Above discontinuity	Below discontinuity	
Propan-2-ol	0	55	17	26	9
	25	54	20	26	6
	55	N.D.	20	21	1
Ethanol	0	48	18	45	27
	25	46	23	43	20
	55	45	21	36	16

for the oxidation of propan-2-ol was linear from 25 to 90 °C when the enzyme was incubated at 55 °C before assay. Under the same conditions, however, a distinct discontinuity was seen in the Arrhenius plot for ethanol oxidation (Figure 4B). Discontinuities were also observed at approx. 55 °C and approx. 46 °C for propan-2-ol and ethanol oxidations respectively when the enzyme was preincubated at 0 or 25 °C (Table 2). The slopes of the best fit regression lines above and below the discontinuity were significantly different beyond the 95% confidence level except for propan-2-ol oxidation by enzyme preincubated at 55 °C, where the regression line slopes were similar at the 95% confidence level. The activation energies for propan-2-ol and ethanol oxidations were similar at assay temperatures above the discontinuities but were 15–20 kJ/mol higher for ethanol oxidation than for propan-2-ol oxidation at temperatures below the discontinuity temperatures (Table 2). Furthermore the differences between activation energies above and below the discontinuity temperatures ( $\Delta$ ) decreased with increasing preincubation temperatures, and the differences for ethanol oxidation were at least 3-fold higher than for propan-2-ol oxidation.

#### DISCUSSION

This first report of the cloning and expression of a thermophilic S-ADH also provides evidence on the molecular bases for enzyme activity, thermophilicity and discontinuous Arrhenius plots. Protein sequence comparisons predict that P-ADHs and S-ADHs have some structure–function similarities related to catalytic Zn and nicotinamide cofactor binding. However, differences in the hydrophobic clusters present in the overall P-ADH and S-ADH sequences predict significant differences in the overall structures of these enzymes. The recombinant *T. ethanolicus* protein, with kinetic properties similar to those of the native enzyme [6], is a thermophilic and thermostable NADP(H)-dependent enzyme that exhibits significantly greater catalytic efficiency towards secondary than primary alcohols owing to both lower  $K_m$  (app) and higher  $V_{\text{max}}$  (app) values. Chemical modification experiments suggest that enzyme activity requires at least Cys and His residues and a tightly bound Zn atom. Finally, the magnitude of the bend in the Arrhenius plots varied inversely with enzyme preincubation temperature, indicating the existence of a catalytically significant, temperature-dependent structural change in the enzyme.

The *adhB* gene encoding the thermophilic *T. ethanolicus* S-ADH was cloned by hybridization and expressed in *E. coli*.

Comparisons of the native and recombinant enzymes' N-terminal sequences and molecular masses showed that the recombinant enzyme differed from the native protein only by the addition of an N-terminal methionine. Although the first ATG is the main translation start codon in *E. coli*, it is unknown whether it is the sole initiation codon (and the first methionine is processed later), or whether the second ATG is also used as an initiation codon. The presence of a truncated ORF (preceded by an RBS) 180 nucleotides downstream of *adhB* and the absence of any potential transcriptional stop signal suggested that *adhB* might be the first gene of an operon. Although confirmation of this hypothesis will require additional experimentation, the similarity between the truncated ORF reported here and the ORF downstream of *C. beijerinckii adhB* lends further support to this hypothesis.

HCA alignments of the P-ADHs and S-ADHs directed by their pyridine dinucleotide binding motifs indicated some structural similarity between these classes of enzyme. The negatively charged Asp<sup>(223,195,215)</sup> residues are consistent with the NAD(H) dependence of the horse liver, *B. stearothermophilus*, and *A. eutrophus* enzymes respectively, whereas the presence of an uncharged residue (Gly<sup>198</sup>) at the analogous position in the *T. ethanolicus*, *T. brockii* and *C. beijerinckii* S-ADHs is consistent with the NADP(H) dependence of these enzymes [3,6,7]. Furthermore, residues identified in the enzyme hydrophobic core, residues lining the active site cavity, and structurally important glycines previously identified in the horse liver P-ADH [1] were better conserved between proteins in this alignment than the overall peptide sequences. Similarity of putative structurally critical regions has been reported for other ADH comparisons [34]. The correlation between enzyme structure–function properties and the predictions of this alignment support its use in further ADH structure–function studies. However, the apparent lack of a structural Zn binding loop in the S-ADHs, the reports of only tetrameric S-ADHs but both tetrameric and dimeric P-ADHs, and the significantly greater similarity between the S-ADHs than between P-ADHs and S-ADHs predicted by HCA comparison also suggests that, although functionally similar, P-ADHs and S-ADHs may be less structurally similar than previously believed.

The thermophilic *T. ethanolicus* 39E S-ADH incubated at 90 °C retained detectable activity for more than 1 h, whereas the mesophilic *C. beijerinckii* S-ADH was completely inactivated within 10 min at 70 °C [6]. Nevertheless these two enzymes shared more than 85% sequence similarity. Nine of the non-conservative substitutions between the subunits of these proteins correspond to prolines in the *T. ethanolicus* enzyme. The similarly thermophilic *T. brockii* S-ADH contains eight of these additional prolines. This difference in proline content between the thermophilic and the mesophilic S-ADHs is consistent with the hypothesis of Matthews et al. [33] concerning the role of prolines in protein stabilization and with the observations by numerous investigators of protein stabilization due to proline insertion [35,36], constrained loop regions [37] and proline substitution into loops [38–40]. The additional prolines in the *T. ethanolicus* S-ADH were either in short putative loop regions or in longer putative loop regions containing multiple prolines, suggesting that the specific placement as well as the number of prolines may be critical to their stabilizing effect. The difference in proline content between the *T. ethanolicus* and *C. beijerinckii* enzymes and their overall high sequence similarity makes these S-ADHs an excellent system for testing the effect of proline insertion on protein structure stabilization.

Comparative sequence analysis predicted the involvement of specific Cys, His and Asp residues in S-ADH catalysis. Chemical modification of the recombinant and native *T. ethanolicus* S-

ADHs with DTNB established the importance of cysteine residues in catalysis. The observation that Zn was the only metal enhancing the enzyme reactivation after DTNB modification suggested that the enzyme is Zn-dependent. This finding is in agreement with the previous report that, once inactivated by the thiol-modifying reagent *p*-chloromercuribenzoate, the *T. brockii* S-ADH recovered activity only in the presence of ZnCl<sub>2</sub> [3]. Here the recovery of 34% of the initial activity on reversal of DTNB modification in the absence of added metal, and the inability of EDTA to reduce the rate of reactivation, even at 60 °C, suggested that the catalytic metal remained tightly bound to the protein. Histidine-specific modification of the *T. ethanolicus* enzyme by DEPC was also accompanied by complete enzyme inactivation, implicating a histidine residue in catalysis. The apparent lack of a structural Zn binding region in the S-ADH subunits argues that the DTNB-linked inactivation and Zn-dependent reactivation are not due to the loss and recovery of a Cys-liganded structural Zn. Therefore the catalytically important Cys and His residues might act as ligands to the catalytic Zn, as described for other ADHs [1]. Determination of the importance of Asp<sup>150</sup> to S-ADH activity awaits mutagenic, crystallographic or physical biochemical analysis.

The temperature dependence of catalytic activities of the native and recombinant enzymes were similar. The Arrhenius plot for propan-2-ol oxidation by *T. ethanolicus* S-ADH preincubated at 55 °C was linear, unlike that previously reported for the *T. brockii* S-ADH [3]. However, statistically significant discontinuities in the Arrhenius plots for both ethanol and propan-2-ol oxidation by the *T. ethanolicus* enzyme were seen when the enzyme was preincubated at lower temperatures. A change in the rate-determining step of the overall reaction and other explanations that do not invoke alterations in catalyst structure predict Arrhenius plot discontinuities [44,45]. A shift in the reaction slow step not related to an alteration in enzyme structure would be independent of the initial temperature of the enzyme, and is inconsistent with the inverse relationship observed here between enzyme preincubation temperature and the difference in activation energies above and below the discontinuity ( $\Delta$ ). At assay temperatures above the discontinuity, the reaction activation energies were similar for enzymes preincubated at 0, 25 and 55 °C, unlike those at lower assay temperatures. This observation is consistent with the enzyme's attaining its optimally active conformation rapidly enough at higher assay temperatures not to affect the measured rate. The discontinuity temperatures, being below the lowest reported temperatures for *T. ethanolicus* growth, are physiologically irrelevant, but they underscore the importance of treating thermophilic enzymes differently from mesophilic enzymes when conducting kinetic analyses. Furthermore the differences between the low temperature activation energies for ethanol and propan-2-ol argue that substrate/product–protein interactions are important to the rate-determining step in catalysis.

The Arrhenius plot was linear for propan-2-ol oxidation by the S-ADH preincubated at 55 °C, arguing that under these conditions the temperature dependence of reaction rate is due predominantly to the change in average substrate molecular energy rather than to a functionally significant structural change. Although these results are not conclusive, the lack of a catalytically significant alteration in enzyme structure, seen as a discontinuity in the Arrhenius plot, makes excessive rigidity (resistance to structural change) of the thermophilic protein unnecessary to explain the low *T. ethanolicus* S-ADH activity at mesophilic temperatures compared with the activity of the mesophilic enzyme [6]. Therefore, although the *T. ethanolicus* S-ADH can undergo a temperature-dependent, catalytically signi-

ficant structural change, a discontinuity in the Arrhenius plot cannot be invoked as evidence for greater thermophilic protein rigidity.

The linear Arrhenius plot for propan-2-ol oxidation by *T. ethanolicus* S-ADH preincubated at 55 °C indicates that the low mesophilic temperature activity of this enzyme might be explained by the substrate energy alone. Arrhenius theory predicts increasing  $K_m$  (app) and  $V_{max}$  (app) with increasing temperature [44], and this effect has been confirmed for the *Thermotoga neopolitana* D-xylose isomerase [46]. The thermophilic S-ADH has lower  $V_{max}$  (app) values than would be predicted from extension of the mesophilic enzyme activity at 25 °C. In fact, at 60 °C the thermophilic S-ADH maintains  $K_m$  (app) and  $V_{max}$  (app) values towards substrates similar to those reported for the mesophilic enzyme at 25 °C. These similar kinetic values suggest that the thermophilic enzyme channels more excess substrate-binding energy into substrate binding and less into turnover [47]. Therefore the *T. ethanolicus* S-ADH seems to maintain substrate affinity at high temperatures by sacrificing high turnover number.

We thank Maris Laivenieks for assistance in protein purification and molecular biology, as well as Dr. Vladimir Tchernajenko and Dr. David Giegel for helpful discussions. The MSU Mass Spectrometry Facility is supported in part by a grant (DRR-00480) from the Biotechnology Resource Technology Program, National Center for Research Resources, National Institutes of Health. This research was supported by a grant from the Cooperative State Research Service, U.S. Department of Agriculture, under the agreement 90-34189-5014.

## REFERENCES

- Brändén, C.-I., Jörnvall, H., Eklund, H. and Furugren, B. (1975) in *The enzymes*, (Boyer, P. D., ed.), vol. XI, part A, pp. 103–190, Academic Press, New York
- Eklund, H., Nordström, B., Zeppezauer, E., Söderlund, G., Ohlsson, I., Boiwe, T. and Brändén, C.-I. (1974) *FEBS Lett.* **44**, 200–204
- Lamed, R. J. and Zeikus, J. G. (1981) *Biochem. J.* **195**, 183–190
- Steinbüchel, A. and Schlegel, H. G. (1984) *Eur. J. Biochem.* **141**, 555–564
- Bryant, F. O., Wiegel, J. and Ljungdahl, L. (1988) *Appl. Env. Microbiol.* **54**, 460–465
- Ismail, A. A., Zhu, C.-X., Colby, G. D. and Chen, J.-S. (1993) *J. Bacteriol.* **175**, 5097–5105
- Burdette, D. S. and Zeikus, J. G. (1994) *Biochem. J.* **302**, 163–170
- Lovitt, R. W., Shen, G.-S. and Zeikus, J. G. (1988) *J. Bacteriol.* **170**, 2809–2815
- Keinan, E., Hafeli, E. K., Seth, K. K. and Lamed, R. L. (1986) *J. Am. Chem. Soc.* **108**, 162–169
- Keinan, E., Hafeli, E. K., Seth, K. K. and Lamed, R. L. (1986) *Ann. N. Y. Acad. Sci.* **501**, 130–149
- Hummel, W. (1990) *Appl. Microbiol. Biotechnol.* **34**, 15–19
- Keinan, E., Seth, K. K., Lamed, R. L., Ghirlando, R. and Singh, S. P. (1990) *Biocatalysis* **4**, 1–15
- Hummel, W. and Kula, M.-R. (1989) *Eur. J. Biochem.* **184**, 1–13
- Persson, M., Månsson, M.-O., Bülow, L. and Mosbach, K. (1991) *Biotechnology* **9**, 280–284
- Lee, Y.-E., Jain, M. K., Lee, C., Lowe, S. E. and Zeikus, J. G. (1993) *Int. J. Syst. Bacteriol.* **43**, 41–51
- Nagata, N., Maeda, K. and Scopes, R. K. (1992) *Bioseparation* **2**, 353–362
- Peretz, M. and Burstein, Y. (1989) *Biochemistry* **28**, 6549–6555
- Oka, A., Sugisaki, H. and Takanami, M. (1981) *J. Mol. Biol.* **147**, 217–226
- Zeikus, J. G., Hegge, P. W. and Anderson, M. A. (1979) *Arch. Microbiol.* **122**, 41–48
- Sambrook, J., Fritsch, E. F. and Maniatis, T. (1989) in *Molecular Cloning: A Laboratory Manual*, 2nd edn. (Nolan, C., ed.), Cold Spring Harbor Press, Cold Spring Harbor, NY
- Ausubel, F. M., Brent, R., Kingston, R. E., Moore, D. D., Seidman, J. G., Smith, J. A. and Struhl, K. (1993) in *Current Protocols in Molecular Biology* (Janssen, K., ed.), Current Protocols, New York
- Doi, R. H. (1983) in *Recombinant DNA Techniques: An Introduction* (Rodriguez, R. L. and Tait, R. C., eds.), pp. 162–163, Benjamin-Cummings, Menlo Park, CA
- Lee, C. C., Wu, X., Gibbs, R. A., Cook, R. G., Muzny, D. M. and Caskey, C. T. (1988) *Science* **239**, 1288–1291
- Sanger, F., Nicklen, S. and Coulson, A. R. (1977) *Proc. Natl. Acad. Sci. U.S.A.* **74**, 5463–5467
- Brooks, S. (1992) *Biotechniques* **13**, 906–911
- Smith, P. K., Krohn, R. I., Hermanson, G. T., Mallia, A. K., Gartner, F. H., Provenzano, M. D., Fugimoto, E. K., Goele, N. M., Olson, B. J. and Klenk, D. C. (1985) *Anal. Biochem.* **150**, 76–85
- Remington, R. D. and Schork, M. A. (1985) in *Statistics with Applications to the Biological and Health Sciences*, pp. 296–309, Prentice-Hall, Englewood Cliffs, NJ
- Habeeb, A. F. S. A. (1972) *Methods Enzymol.* **25B**, 457–459
- Miles, E. W. (1977) *Methods Enzymol.* **47**, 431–442
- Lemesle-Verloot, L., Henrissat, B., Gaboriaud, C., Bissery, V., Morgat, A. and Mornon, J. P. (1990) *Biochimie* **72**, 555–574
- Hawley, D. K. and McClure, W. R. (1983) *Nucleic Acids Res.* **11**, 2237–2255
- Wierenga, R. K. and Hol, G. J. (1983) *Nature (London)* **302**, 842–844
- Matthews, B. W., Nicholson, H. and Becktel, W. (1987) *Proc. Natl. Acad. Sci. U.S.A.* **84**, 6663–6667
- Jendrossek, D., Steinbuechel, A. and Schlegel, H. G. (1988) *J. Bacteriol.* **170**, 5248–5256
- Herning, T., Katsuhide, Y., Taniyama, Y. and Kikuchi, M. (1991) *Biochemistry* **30**, 9882–9891
- Herning, T., Katsuhide, Y., Inaka, K., Matsushima, M. and Kikuchi, M. (1992) *Biochemistry* **31**, 7077–7085
- Eijsink, V. G. H., Vriend, G., van de Burg, B., van de Zee, J. R., Veltman, O. R., Stulp, B. K. and Venema, G. (1993) *Protein Eng.* **5**, 157–163
- Watanabe, K., Masuda, T., Ohashi, H., Mihara, H. and Suzuki, Y. (1994) *Eur. J. Biochem.* **226**, 277–283
- Watanabe, K., Chishiro, K., Kitamura, K. and Suzuki, Y. (1991) *J. Biol. Chem.* **266**, 24287–24294
- Hardy, F., Vriend, G., Veltman, O. R., van de Vinne, B., Venema, G. and Eijsink, V. G. H. (1993) *FEBS Lett.* **317**, 89–92
- Reference deleted
- Reference deleted
- Reference deleted
- Segel, I. H. (1975) in *Enzyme Kinetics: Behavior and Analysis of Rapid Equilibrium and Steady-State Enzyme Systems*, pp. 929–934, John Wiley & Sons, New York
- Londesborough, J. (1980) *Eur. J. Biochem.* **105**, 211–215
- Vieille, C., Hess, J. M., Kelly, R. M. and Zeikus, J. G. (1995) *Appl. Environ. Microbiol.* **61**, 1867–1875
- Jencks, W. P. (1975) *Adv. Enzymol. Relat. Areas Mol. Biol.* **43**, 219–411